Chemical Vapor Deposition of Titanium, Zirconium, and Hafnium Nitride Thin Films

Renaud Fix,[1a] Roy G. Gordon,*[,1a] and David M. Hoffman*[,1b]

Department of Chemistry, Harvard University, Cambridge, Massachusetts 02138, and the Department of Chemistry, University of Houston, Houston, Texas 77204

Received August 12, 1991

Titanium, zirconium, and hafnium nitride thin films were synthesized from tetrakis(dialkylamido)metal(IV) complexes and ammonia by atmospheric pressure chemical vapor deposition with high growth rates at low substrate temperatures (200–450 °C). Depositions were successfully carried out on silicon, low-sodium glass, soda lime glass, vitreous carbon, and boron substrates. Stainless steel and polyester were also used as substrates for depositions of titanium nitride below 250 °C. All of the films showed good adhesion to the substrates and were chemically resistant. The films were characterized by Rutherford backscattering spectrometry, X-ray photoelectron spectroscopy, ellipsometry, and transmission electron microscopy. Reflectance and transmission spectra were also recorded. Hydrogen in the films was estimated by hydrogen forward recoil scattering spectrometry. The titanium nitride coatings were slightly nitrogen-rich TiN (N/M ratio 1.05–1.15). These films displayed metallic properties and were crystalline as deposited. The zirconium and hafnium nitride films were Zr_3N_4 and nitrogen-rich Hf_3N_4 (N/M ratios 1.35 ± 0.05 and 1.7 ± 0.1, respectively). They were crystalline, yellow-colored, transparent, and insulating. The hydrogen content of the films diminished as the deposition temperature increased. For depositions carried out at 400 °C the TiN films contained 9 atom % hydrogen and at 300 °C the Zr_3N_4 and Hf_3N_4 films contained 10 and 16 atom % hydrogen, respectively. The hydrogen is proposed to be incorporated in the films as NH and NH_2 groups in the amorphous portion of a mix composed of amorphous material and imbedded nitride crystallites.

Titanium, zirconium, and hafnium each form a cubic nitride phase of stoichiometry MN.[2] These phases exhibit metallic behavior, extreme hardness, high melting points (ca. 3000 °C), remarkable chemical resistance (e.g., they are inert to organic solvents and inorganic acids), and low-temperature superconductivity.

Because of the properties displayed by the MN compounds, their thin films have many potential applications. For example, they can be used as wear-resistant, friction-reducing coatings for machine tools[3-11] and gold-colored decorative coatings.[9,12] Also, their optical properties make them suitable for use as wavelength-selective transparent optical films and solor control coatings for windows.[13-19] In microelectronic devices, MN films are of use as low-resistance contacts and diffusion barriers in interconnect metallization schemes.[20-35] TiN and ZrN have also been proposed for use in low-barrier Schottky diodes and as the gate electrode in MOS transistors.[21,36]

Coatings of the group 4 MN compounds have been prepared by both chemical and physical vapor deposition techniques. For example, tribiological and cosmetic coatings have been prepared by chemical vapor deposition (CVD) from the metal halides, nitrogen, and hydrogen at temperatures above 1000 °C (eq 1).[4-6,13,16,37,38] Gordon and

(1) (a) Harvard University. (b) University of Houston.
(2) Toth, L. E. *Transition Metal Carbides and Nitrides*; Margrave, J. L., Ed.; Refractory Materials, Vol. 7; Academic Press: New York, 1971.
(3) Hintermann, H. E. *Oberflaeche-Surf.* **1981**, *22*, 224.
(4) Schintlmeister, W.; Pacher, O.; Pfaffinger, K.; Raine, T. *J. Electrochem. Soc.* **1976**, *123*, 924.
(5) Schintlmeister, W.; Pacher, O.; Krall, T.; Wallgram, W.; Raine, T. *Powder Metall. Int.* **1981**, *13*, 71.
(6) Hintermann, H. E. *Thin Solid Films* **1981**, *84*, 215.
(7) Münz, W. D.; Hofmann, D. Hartig, K. *Thin Solid Films* **1982**, *96*, 79.
(8) Molarius, J. M.; Korhonen, A. S.; Ristolainen, E. O. *J. Vac. Sci. Technol. A* **1985**, *3*, 2419.
(9) Hirose, M.; Yasui, T.; Ochi, Y.; Nakagawa, M. U.S. Patent 4,420,498.
(10) Johnson, P. C.; Randhawa, H. *Surf. Coat. Technol.* **1987**, *33*, 53.
(11) Johansson, B. O.; Sundren, J.-E.; Helmersson, U.; Hibbs, M. K. *Appl. Phys. Lett.* **1984**, *44*, 670.
(12) Buhl, R.; Pulker, H. K.; Moll, E. *Thin Solid Films* **1981**, *80*, 265.
(13) Karlsson, B.; Shimshock, R. P.; Seraphin, B. O.; Haygarth, J. C. *Solar Energy Mater.* **1983**, *7*, 401.
(14) Valkonen, E.; Karlsson, T.; Karlsson, B.; Johannson, B. O. *Thin Film Technol. Proc. Soc. Photo-Opt. Instrum. Eng.* **1983**, *401*, 375.
(15) Karlsson, B.; Ribbing, C. G. *Optical Coatings for Energy Efficiency and Solar Applications, Proc. SPIE* **1982**, *342*, 52.
(16) Schlegel, A.; Wachter, P.; Nickl, J. J.; Lingg, H. *J. Phys. C: Solid State Phys.* **1977**, *10*, 4889.
(17) Erola, M.; Keinonen, J.; Anttila, A.; Koskinen, J. *Solar. Energy. Mater.* **1985**, *12*, 353.
(18) Kurtz, S. R.; Gordon, R. G. *Thin Solid Films* **1986**, *140*, 277.
(19) Solnyshko, L. N.; Chistyi, I. L.; Drobot, A. D.; Yampol'skii, V. I.; Egorov, V. N. *Sov. J. Opt. Technol. (Engl. Transl.)* **1981**, *48*, 562; *Opt. Mekh. Promst.* **1981**, *48*, 53.
(20) Gupta, S.; Song, J.-S.; Ramachandran, V. *Semiconduct. Int.* **1989**, *12* (11), 80.
(21) Wittmer, M.; Studer, B.; Melchior, H. *J. Appl. Phys.* **1981**, *52*, 5722.
(22) Ernsberger, C.; Nickerson, J.; Miller, A.; Banks, D. *J. Vac. Sci. Technol. A* **1985**, *3*, 2303.
(23) Suni, I.; Mäenpää, M.; Nicolet, M.-A.; Luomajärvi, M. *J. Electrochem. Soc.* **1983**, *130*, 1215.
(24) Mäenpää, M.; Suni, I.; Sigurd, D.; Finetti, M.; Nicolet, M.-A. *Phys. Status Solidi A* **1982**, *72*, 763.
(25) Cheung, N.; Seefeld, von H.; Nicolet, M.-A. In *Proc. Symp. on Thin Film Interfaces and Interactions*; Baglin, J. E. E., Poate, J. M. Eds.; The Electrochemcal Society Proceedings 802; The Electrochemical Society: Princeton, 1980; p 323.
(26) Mäenpää, M.; Nicolet, M.-A.; Suni, I.; Colgan, E. G. *Solar Energy* **1981**, *27*, 283.
(27) Seefeld, von H.; Cheung, N. W.; Mäenpää, M.; Nicolet, M.-A. *IEEE Trans. Electron Devices* **1980**, *ED-27*, 873.
(28) Kanamori, S.; Matzumoto, T. *Thin Solid Films* **1983**, *110*, 205.
(29) Ting, C. Y. *J. Vac. Sci. Technol.* **1982**, *21*, 14.
(30) Schutz, R. J. *Thin Solid Films* **1983**, *104*, 89.
(31) Mändl, M.; Hoffmann, H.; Kücher, P. *J. Appl. Phys.*, in press.
(32) Raaijmakers, I. J.; Sherman, A. *Proceedings of the 7th International IEEE VLSI Multilevel Interconnection Conference*, in press.
(33) Yokoyama, N.; Hinode, K.; Homma, Y. *J. Electrochem. Soc.* **1989**, *136*, 882.
(34) Noël, J.-P.; Houghton, D. C.; Este, G.; Shepherd, F. R.; Plattner, H. *J. Vac. Sci. Technol. A* **1984**, *2*, 284.
(35) Hems, J. *Semiconduct. Int.* **1990**, *13* (12), 100.
(36) Wittmer, M. *J. Vac. Sci. Technol.* **1985**, *3*, 1797.

0897-4756/91/2803-1138$02.50/0

$$MCl_4 + \tfrac{1}{2}N_2 + 2H_2 \xrightarrow{>1000\ °C} MN + 4HCl \quad (M = Ti, Zr, Hf) \quad (1)$$

Kurtz[18] showed that substitution of the N_2/H_2 mixture by ammonia, a more reactive nitrogen source, significantly lowered the deposition temperature (550 °C) of TiN (eq 2). Substitution of ammonia had a lesser effect on the deposition temperatures of ZrN and HfN (800–900 °C).[13,16]

$$6TiCl_4 + 8NH_3 \xrightarrow{500\text{–}700\ °C} 6TiN + 24HCl + N_2 \quad (2)$$

The temperatures required for these CVD reactions are not compatible with thermally sensitive substrates, such as those used in the processing of semiconductor components (e.g., aluminized silicon chips and amorphous silicon solar cells). For depositions involving delicate substrates, physical vapor deposition (PVD) techniques such as sputtering or reactive evaporation have been preferred for the preparation of MN films.[20–31,34–36]

Some physical deposition techniques (ion beam deposition,[39,40] triode ion plating,[41–44] reactive sputtering,[19,45–50] and ion implantation)[51] have also allowed the preparation of group 4 nitride films with N/M ratios greater than 1. Salmenoja and co-workers, for example, have prepared titanium nitride with a N/M ratio as high as 1.5 by triode ion plating,[42] and Johansson and co-workers have prepared zirconium and hafnium nitrides with N/M ratios of 1.75 and 2.13, respectively, by dual ion beam deposition.[39] For N/M ratios greater than 1.2, zirconium and hafnium nitride phases of stoichiometry M_3N_4 were produced.[11,39–41,45] The M_3N_4 phases were transparent and insulating in contrast to nitrogen-rich TiN, which was reported to be a dark conductive material with no apparent structural change from stoichiometric TiN; that is, there does not appear to be a stable Ti_3N_4 phase.[39,41,45] Transparent or insulating titanium nitride films have not been reported.

The zirconium and hafnium M_3N_4 phases were proposed to be related to the MN phase by a rhombohedral distortion. Because of the close lattice match between the MN and M_3N_4 phases, Schwartz and co-workers have postulated that Zr_3N_4 could be the basis for new high-T_c NaCl-type superconductors[51] and isostructural, isochemical, and all refractory $ZrN/Zr_3N_4/ZrN$ Josephson junction devices.[52] Solnyshko and co-workers showed that ZrN_x can also be used as an interference coating for near-IR radiation.[19]

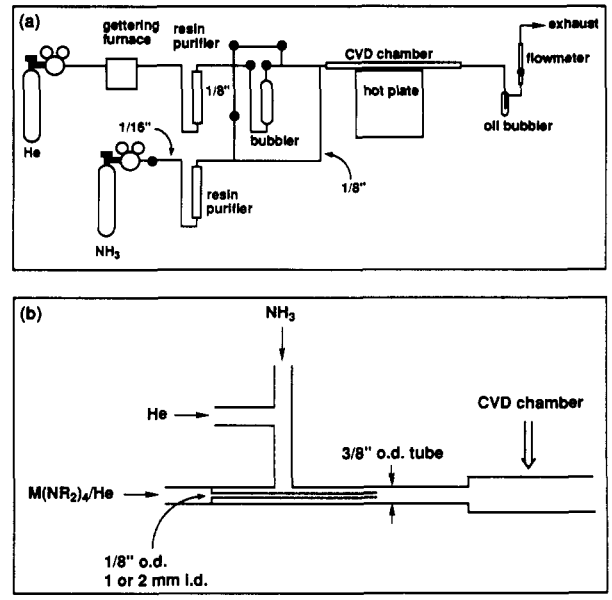

Figure 1. (a) Schematic of the experimental APCVD apparatus. All tubing was $^1/_4$ in. unless otherwise indicated. (b) Schematic of the reactor inlet lines.

Thin films of the M_3N_4 compounds have not been prepared by chemical routes, although Zr_3N_4 in powder form was first identified by Juza and co-workers in 1964 as a product of the reaction between ZrI_4 and ammonia at 750 °C,[53,54] and powdered mixtures containing some Zr_3N_4 were later obtained from $ZrCl_4$ and NH_3 at 900 °C.[55,56]

Because CVD has several advantages over PVD, including generally better step coverage, denser films, higher growth rates, and better control of morphology, microstructure, and stoichiometry, there is a clear need to develop CVD routes to the M_3N_4 phases. Also, lower temperature routes to the MN phases are necessary so that more delicate substrates can be accommodated. As mentioned, previous attempts to lower the depositon temperature of MN (M = Ti, Zr, Hf) films involved the use of ammonia as the nitrogen source rather than N_2/H_2 in reactions with MCl_4. The present study focuses on a more reactive class of metal-containing precursors than the chlorides; namely, tetrakis(dialkylamido)metal complexes.

Our choice of the homoleptic amido complexes as precursors was prompted by solution reactivity studies carried out by Bradley and co-workers in the early 1960s. They reported that dialkylamido complexes underwent facile transamination reactions in solution (eq 3).[57] With primary amines, reaction 3 led to imido-bridged oligomers when the akyl substituent was small (eq 4)[58,59] and to dimer

$$M\text{–}NR_2 + HNR'_2 \rightarrow M\text{–}NR'_2 + HNR_2 \quad (3)$$

$$M(NMe_2)_4 + RNH_2 \rightarrow [M(=NR)_2]_x + HNMe_2 \quad (M = Ti, Zr) \quad (4)$$

$$2M(NMe_2)_4 + 2t\text{-}BuNH_2 \rightarrow [M_2(NMe_2)_2(\mu\text{-}N\text{-}t\text{-}Bu)]_2 + 4HNMe_2 \quad (5)$$

(37) Itoh, H.; Kato, K.; Sugiyama, K. *J. Mater. Sci.* **1986**, *21*, 751.
(38) Kim, M. S.; Chun, J. S. *Thin Solid Films* **1983**, *107*, 129.
(39) Johansson, B. O.; Hentzell, H. T. G.; Harper, J. M. E.; Cuomo, J. J. *J. Mater. Res.* **1986**, *1*, 442.
(40) Netterfield, R. P.; Martin, P. J.; McKenzie, D. R. *J. Mater. Sci. Lett.* **1990**, *9*, 972.
(41) Ristolainen, E. O.; Molarius, J. M.; Korhonen, S. A.; Lindroos, V. K. *J. Vac. Sci. Technol. A* **1987**, *5*, 2184.
(42) Salmenoja, K.; Korhonen, A. S.; Erola, E.; Molarius, J. M. *Appl. Phys. Lett.* **1986**, *49*, 505.
(43) Salmenoja, K.; Korhonen, A. S. *Vacuum* **1986**, *36*, 33.
(44) Salmenoja, K.; Korhonen, A. S.; Sulonen, M. S. *J. Vac. Sci. Technol. A* **1985**, *3*, 2364.
(45) Yee, D. S.; Cuomo, J. J.; Frisch, M. A.; Smith, D. P. E. *J. Vac. Sci. Technol. A* **1986**, *4*, 381.
(46) Cuomo, J. J.; Leary, P. A.; Yu, D.; Reuter, W.; Frisch, M. *J. Vac. Sci. Technol.* **1979**, *16*, 299.
(47) Lemperière, G.; Poitevin, J. M. *Thin Solid Films* **1984**, *111*, 339.
(48) Aron, P. R.; Grill, A. *Thin Solid Films* **1982**, *96*, 87.
(49) Smith, F. T. J. *J. Appl. Phys.* **1970**, *41*, 4227.
(50) Anttila, A.; Keinonen, J.; Uhrmacher, M.; Vahvaselkä, S. *J. Appl. Phys.* **1985**, *57*, 1423.
(51) Schwartz, K.; Yee, D. S.; Cuomo, J. J.; Harper, J. M. E. *Phys. Rev. B: Condens. Matter* **1985**, *32*, 5419.
(52) Schwarz, K.; Williams, A. R.; Cuomo, J. J.; Harper, J. H. E.; Hentzell, H. T. G. *Phys. Rev. B: Condens. Matter* **1985**, *32*, 8312.
(53) Juza, R.; Rabenau, H.; Nitschke, I. *Z. Anorg. Allg. Chem.* **1964**, *332*, 1.
(54) Juza, R.; Gabel, A.; Rabenau, H.; Klose, W. *Z. Anorg. Allg. Chem.* **1964**, *329*, 136.
(55) Yajima, A.; Segawa, Y.; Matsuzaki, R.; Saeki, Y. *Bull. Chem. Soc. Jpn.* **1983**, *56*, 2638.
(56) Orlovskii, V. P.; Rudenko, N. V.; Ivanov-Emin, B. N. *Russ. J. Inorg. Chem.* **1967**, *12*, 1217.
(57) Bradley, D. C.; Thomas, I. M. *J. Chem. Soc.* **1960**, 3857.
(58) Bradley, D. C.; Torrible, E. G. *Can. J. Chem.* **1963**, *41*, 134.
(59) Bartlett, R. K. *J. Inorg. Nucl. Chem.* **1966**, *28*, 2448.

formation in the case of t-$BuNH_2$ (eq 5).[58,60] The formation of formal M–N multiple bonds by successive amine elimination reactions in eqs 4 and 5 suggested to us that a combination of transamination and amine elimination reactions involving volatile metal amido complexes could be the basis for the CVD synthesis of metal nitride thin films if ammonia were the coreactant.

Herein we show that the kinetically facile solution processes illustrated by eqs 3–5 are applicable to a CVD system by synthesizing thin films of M_3N_4 (M = Zr, Hf) and TiN from $M(NR_2)_4$ and ammonia precursors at low temperatures.[61]

Experimental Section

The compounds $Ti(NMe_2)_4$,[57] $Zr(NEt_2)_4$,[57] and $Hf(NEt_2)_4$[62] were synthesized as described by Bradley and co-workers.

The CVD experimental apparatus, schematically illustrated in Figure 1a, consisted of an inert carrier gas delivery assembly, an ammonia delivery line, a precursor handling system, and a reactor. The parts are described below.

Inert Gas and Ammonia Delivery Systems. The inert-gas delivery system supplied the helium carrier gas used for the transport of the organometallic precursor and dilution of ammonia. It also had components that purified the commercial gases.

The gas lines were primarily 0.25-in. oxygen-polished stainless steel tubing (Analabs) connected with welded VCR fittings. To decrease the possibility of leaks, the number of connector fittings was kept to a minimum in the design. Sections of small-diameter tubing (see Figure 1) limited the gas-flow rate, which was further adjusted by use of a gas pressure regulator valve (pressure setting of 0–5 psig). The gas flow was measured at the exhaust of the CVD chamber with a rotameter. The inert gas regulator was a Matheson high-purity model (No. 3803) equipped with a metal seat. It was connected to the cylinder via a cross purge assembly.

The carrier gas was purified by passing it first through a gettering furnace and then a resin-type purifier. The gettering furnace was a Matheson Hydrox purifier (Model 8301) containing a Ti–Zr alloy. This alloy, which was maintained at 500 °C, removed oxygen, moisture, carbon dioxide, and nitrogen from the helium stream. The purifier was rated by the manufacturer to produce an outflow containing less than 0.1 ppm of oxygen and 0.1 ppm of water. The resin-based purifier was from Nanochem (Hercules, Model L-50 t, resin type IV). It was rated by the manufacturer to remove oxygen and water to the ppb level. The gas stream that exited from the Nanochem purifier was divided such that one half was directed into a bubbler assembly and the other half into the ammonia line, where it was used to dilute the ammonia. The ammonia was obtained from Matheson (USLI grade) and had a rated total purity of 99.9995%. It was purified further by passing it through a separate Nanochem resin-type purifier (Model L-50 t, resin type 1400).

Organometallic Precursor Handling System. The organometallic precursor handling system consisted of a bubbler and a bypass line. The precursor was loaded into a stainless steel U-shaped container (the "bubbler") equipped with two bellows valves. The bypass line allowed continuous purging of the CVD chamber before and after deposition. During deposition the bypass line was closed and the bubbler valves were open, which directed the flow of carrier gas through the bubbler.

Heating tape was used to heat the bubbler assembly, thereby increasing the precursor vapor pressure. The bubbler temperature was controlled with a Dynasense proportional controller. A Pt probe wrapped under the heating tape in contact with the bubbler was used to monitor the temperature. The resolution of the temperature control was ±2 °C but the actual temperature of the precursor was undoubtedly lower.

CVD Reactor. The reactor was made from glass. It was rectangularly shaped (1 cm × 4 cm × 1.5 ft) with heat applied from below. A nickel block was placed between the glass reactor and the hot plate, thereby allowing uniform heat distribution.

The reactor was heated from two sources. The primary heat source was a Corning hot plate equipped with a remote controller and the auxiliary heat source was a high-temperature heating tape (Samox) wrapped around the nickel block, which was regulated with a proportional controller. The temperature was monitored by use of a Pt probe placed in a cavity that had been drilled in the nickel plate approximately $^1/_8$ in. from the top surface. The hot plate and nickel block were surrounded by Ceramfab insulating blocks.

The hot plate was used to provide fast heating of the reactor. Once the desired approximate temperature range was achieved, the hot plate was either turned off (for temperatures below 350 °C) or kept on a low setting (for temperatures above 400 °C). Fine tuning of the temperature was then accomplished by use of the heating tape connected to the proportional controller. There was a horizontal temperature gradient of about 10 °C from the edge of the hot plate to the center. This effect was not important, however, because in different runs the substrates were always located at the same location near the reactor inlet.

Ceramfab insulation materials were used to cover the top of the reactor and the exposed surface of the hot plate. This limited the vertical temperature gradient to approximately 10–50 °C.

Concentric inlet lines as illustrated in Figure 1b were used to inject the precursors into the reactor. During depositions, helium was passed through the stainless steel bubbler and the outflow, which was a mixture of the volatilized precursor and helium, then flowed through a 1- or 2-mm-i.d. delivery line into the reaction chamber. Approximately 5 cm before this delivery line entered the reaction chamber, the $M(NR_2)_4$/He mixture was combined with ≈10% ammonia diluted in helium. The combined mixtures passed through a $^3/_8$-in. tube before flowing over the hot substrate. The length of the metal precursor delivery line was tailored to allow proper mixing and to decrease the loss of precursor to powder formation. The diameter of this delivery line also affected film growth (see below).

A glass flange was attached with a clamp at the reactor exhaust. This flange was connected to an oil bubbler to prevent back flow of air into the system. A rotameter was attached after the oil bubbler to control total gas flow.

Depositions. To displace air and moisture, the CVD system, loaded with the substrates, was purged with helium for at least 12 h at 400 °C before the first deposition. Simultaneously the feed lines were baked at 120 °C. Under these conditions, analysis of the helium outflow typically indicated that it contained less than 50 ppb O_2 and H_2O. Subsequent depositions in a series were carried out after 1 h of purging. After each deposition the films were allowed to cool slowly in the reactor under a flow of helium.

During a typical deposition, the precursor was heated to its vacuum (ca. 0.1 mmHg) distillation or sublimation temperature. At this temperature growth rates were maximized with minimal precursor degradation. The ammonia and the organometallic precursor/He delivery lines to the CVD chamber were heated with heating tape to a temperature 20 °C above the temperature at which the stainless steel bubbler was maintained in order to prevent condensation of the precursor and clogging of the reactor inlet.

Film deposition occurred on the substrates and the walls of the reactor. Powder accumulated on the walls of the reactor as well. After a few runs the material on the inside walls of the glass reactor became so thick that the reactor was no longer transparent. This coating was beneficial because it acted as a barrier to oxygen and moisture diffusion from the reactor walls. Occasionally, however, some powder from the top of the reactor would fall on the growing film. A light cleaning was therefore required to remove the poorly adherent material from the reactor. The cleaning was performed in such a way so as to remove the powder stuck on the glass walls but leave as much of the film as possible. Soaking the reactor in dilute $HF:H_2O$ (1:10) followed by rinsings with deionized water and high-purity isopropyl alcohol was found to be suitable for this purpose.

(60) Nugent, W. A.; Harlow, R. L. *Inorg. Chem.* **1979**, *18*, 2030.

(61) A portion of this work has been communicated. See: Fix, R.; Gordon, R. G.; Hoffman, D. M. *Mater. Res. Soc. Symp. Proc.* **1990**, *168*, 357. Fix, R.; Gordon, R. G.; Hoffman, D. M. *J. Am. Chem. Soc.* **1990**, *112*, 7833. For related work concerning main-group nitrides, see: Gordon, R. G.; Hoffman, D. M.; Riaz, U. *Chem. Mater.* **1990**, *2*, 480. Gordon, R. G.; Hoffman, D. M.; Riaz, U. *J. Mater. Res.* **1991**, *6*, 5. Gordon, R. G.; Hoffman, D. M.; Riaz, U. *Mater. Res. Soc. Symp. Proc.* **1991**, *204*, 95.

(62) Bradley, D. C.; Gitlitz, M. H. *J. Chem. Soc. A* **1969**, 980.

Substrate Preparation. Silicon. Crystalline silicon (c-Si) wafers were the primary substrates because silicon was compatible with most film analyses. The only requirement for selecting the wafer was that it had a polished planar surface. The wafers were usually test-grade solid-solubility antimony-doped (n-type) or boron-doped (p-type) 4-in. diameter wafers obtained from Silicon Sense, Andover, MA. The highly polished surface of the wafers had a 100 orientation. Prior to deposition, the silicon substrates were degreased by immersing them in H_2O_2:H_2SO_4 (1:4) for 10 min and then rinsing with deionized water for 10 min.

Glass. Glass substrates permitted the evaluation of the optical and electrical properties of the films. Glass cleaning was more difficult than for c-Si. Two procedures were used to clean the soda lime glass substrates; one is identical with the procedure used for c-Si wafers and the other consisted of a HF/HNO_3 (1:10) treatment followed by exhaustive H_2O rinsings.

Boron and Vitreous Carbon. Vitreous carbon and boron substrates, which were obtained from Atomergic Chemetals Corp., were excellent substrates for light element analysis in Rutherford backscattering spectrometry because of their low atomic number (see below). The vitreous carbon substrates were low-porosity amorphous carbon square plates 2 mm thick. The boron substrates were disks (2 mm thick) that had been cut with a diamond saw from a polycrystalline boron rod (4 mm diameter, 3 cm long). The disks were polished with a diamond wheel.

The boron and vitreous carbon substrates were prepared for depositions by sonicating them in and then rinsing with the following solvents (in order): acetone, $C_2F_3Cl_3$, acetone, high-purity isopropyl alcohol.

The use of vitreous carbon and boron substrates frequently gave higher levels of oxygen contamination in the films than when other types of substrates were employed. This was probably due to H_2O and/or O_2 desorption from the substrate when heated. To minimize this effect, these substrates were baked at 450 °C in the reactor under helium flow for 10 h before the film deposition.

Stainless Steel and Plastic. Stainless steel substrates, which when purchased were covered with a protective tape, were washed with isopropyl alcohol. They were then soaked for 1 min in H_2O_2:H_2SO_4 (1:4) to remove any residue left by the protective plastic tape and then rinsed with water. Plastic substrates were washed with water followed by isopropyl alcohol. The plastic substrates required long purge times before deposition to ensure complete degassing (as indicated by analyzing for O_2 in the outflow gas).

Film Adhesion. Film adhesion to the substrates was tested by two methods.[63] One involved stripping away a piece of adhesive tape (Scotch tape) from the coated substrate. If the film remained on the substrate, it was considered to show "good adhesion". Since this method was rapid and reliable, it was routinely used for all new coatings.

A second method consisted of dipping a coated substrate in liquid nitrogen and, once cold, throwing it on a hot plate kept at 300 °C, and then dipping it again in liquid nitrogen. If the film had not fallen off after repeating this operation 100 times, it was concluded that the film showed good adhesion. This technique was time consuming, and it was used only to test the adhesion of TiN deposited at 200, 300, and 400 °C on silicon.

Mica. Samples for transmission electron microscopy (TEM) were prepared by evaporating films of carbon about 10 nm thick onto freshly cleaved mica substrates. After depositing the metal nitride film onto the carbon-coated mica, the sample was immersed in water to release flakes of film which were then captured on a TEM grid.

Film Characterization. Rutherford backscattering spectrometry (RBS) analyses (General Ionics Model 4117) were carried out by using a beam of 2.0-MeV He^+ for films deposited on silicon and vitreous carbon and 1.8-MeV He^+ for films deposited on boron. (It should be noted that boron gives a nuclear reaction with He^+ at a nuclear resonance of 2.06 MeV).[64] Data analyses were carried out with the program SPECTRUM ANALYSIS.[65]

The hydrogen content of the films was estimated by forward recoil spectrometry (FRS). FRS is a variation of the RBS technique.[66,67] He^+ particles are not backscattered by hydrogen nuclei because of the low mass of the latter and thus hydrogen cannot be detected by RBS. Hydrogen nuclei, however, are recoiled after being hit by a heavier ion such as He^+. FRS, also called elastic recoil detection, is a method for hydrogen quantitative analysis based on the elastic scattering of hydrogen nuclei.

The experimental setup for FRS was similar to RBS, except that the incident beam arrived at a glancing angle (15°) with respect to the sample. In this configuration the detector and the incident beam were at an angle of 150°. A 2.0-MeV He^+ beam was used for the FRS experiments. A thin polyester (Mylar) film (10 μm) was mounted as an absorber in front of the detector in order to stop the flux of elastically scattered He^+ particles.

Each FRS data collection was carried out until a charge of 9.9 μC was accumulated (about 10–15 min). The sample area probed by the beam was an oval about 4 mm long and 1 mm wide. A flat piece of gypsum, $CaSO_4 \cdot 2H_2O$, was used as a calibration standard.[67] Data analysis was carried out by using the program RUMP.[68] The same hydrogen scattering cross section was assumed for all samples. Hydrogen amounts were not corrected for the hydrogen in hydrocarbons that may have been adsorbed on the sample surfaces. No hydrogen depletion was observed during data collection, but the gypsum piece suffered beam damage after prolonged exposure. The number of counts obtained during data collection was reproducible to ±5%.

X-ray photoelectron spectroscopy (XPS) was carried out by using a Surface Science Lab SSX-100 system equipped with a 3-keV Ar^+ sputter gun. The electron-energy analyzer was calibrated to the Au $4f_{7/2}$ line at 84 eV. XPS depth profiles were collected in the unscanned mode by using the monochromatized Al Kα excitation with a spot size 600 μm and the electron-energy analyzer set for a pass energy of 150 eV. The experimental detector width was 18.6 eV in this configuration. The base pressure was 10^{-7} Torr with the Ar^+ gun on. After removing the oxide layer by sputtering, higher resolution spectra for the metal and nitrogen signals were collected in the scanned mode (20-eV window) with a spot size of 300 μm and a pass energy of 50 eV. In this configuration the Ar^+ gun was off during the data acquisition, and the base pressure was less than 10^{-8} Torr. Because of charging problems, insulating zirconium and hafnium nitride films were exposed to a 2.0-eV electron beam charge neutralizer during data collection. The binding energies of these insulating samples were referenced to the surface carbon 1s line set at 284.6 eV.

Transmission electron micrographs and electron diffraction patterns were obtained on a Philips EM420T scanning transmission electron microscope (120 kV).

Results

Film Growth. Titanium, zirconium, and hafnium nitride thin films were grown when ammonia and $Ti(NMe_2)_4$,[57] $Zr(NEt_2)_4$,[57] or $Hf(NEt_2)_4$,[62] respectively, were passed over hot substrates at temperatures in the range 200–450 °C. Titanium nitride was also deposited at 150 °C. Depositions were successfully carried out on silicon, low-sodium glass, soda lime glass, vitreous carbon, and boron substrates. Stainless steel and polyester were also used as substrates for depositions of titanium nitride below 250 °C. When the ammonia reagent was omitted in control experiments, no deposition was observed from any of the organometallic precursors below 350 °C and at this temperature only powdery coatings were obtained.[69–71]

(63) For a review on thin-film adhesion measurements, see: Jacobsson, R. J. *Thin Solid Films* **1976**, *34*, 191.

(64) Lee, Jr., L. L.; Schiffer, J. P. *Phys. Rev.* **1959**, *115*, 160.

(65) RBS data analyses were performed using SPECTRUM ANALYSIS written by Patrick M. Smith, Division of Applied Sciences, Harvard University. Spectrum Analysis is a Fortran program based on algorithms from: Chu, W. K.; Mayer, J. W.; Nicolet, M. A. *Backscattering Spectrometry*; Academic Press: New York, 1978.

(66) Feldman, L. C.; Mayer, J. W. *Fundamentals of Surfaces and Thin Film Analysis*; North-Holland: New York, 1986.

(67) Turos, A.; Meyer, O. *Nucl. Instrum. Methods* **1984**, *B4*, 92.

(68) RUMP is RBS modeling software based on: Doolittle, L. R. *Nucl. Instrum. Methods* **1985**, *B9*, 344.

Table I. Typical CVD Conditions and Film Growth Rates

precursors	bubbler temp, °C	delivery line i.d., mm	He flow, L/min	deposition temp, °C	growth rate,[a] Å/min
$Ti(NMe_2)_4$/ NH_3	25	1	1.5	200	300
$Ti(NMe_2)_4$/ NH_3	55	1	1.5	150–450	2000
$Ti(NMe_2)_4$/ NH_3	55	2	1.5	200–400	2000
$Zr(NEt_2)_4$/ NH_3	100	1	2.5	200	200
$Zr(NEt_2)_4$/ NH_3	120	1	2.5	200–400	500
$Zr(NEt_2)_4$/ NH_3	120	2	2.5	200–400	1500
$Hf(NEt_2)_4$/ NH_3	130	1	1.5	200–430	500
$Hf(NEt_2)_4$/ NH_3	130	2	1.5	200–400	5000

[a] Film thicknesses obtained from RBS analyses.

Generally, the deposits were smooth, nonporous, and pinhole-free and adhered well to all substrates when tested with tape. No peeling or other damage was observed for titanium nitride films deposited at 200, 300, and 400 °C on silicon when they were repeatedly subjected to extreme cold (−198 °C) and heat (300 °C). Scrupulous substrate cleaning and degreasing were critical for good adhesion of films deposited below 300 °C, however. All of the films resisted scratching and abrasion during routine handling. Titanium, zirconium, and hafnium nitride films 1000–3000 Å thick deposited on silicon at 200, 300, and 400 °C were not damaged (as judged by visual inspection) when placed in concentrated HCl and aqua regia for approximately 10 min. In concentrated HF, however, the films appeared to lift off of the substrates.

Titanium nitride coatings were mirrorlike with a reflected gold color when the films were less than 500 Å thick. Thicker coatings (ca. 2000 Å) were entirely absorbing with a silvery appearance. In contrast, the zirconium and hafnium nitride coatings were transparent (even for coatings 5000 Å thick) with a strawlike yellow color and the films deposited on silicon showed the highly colored interference patterns typically observed for insulating coatings with high refractive indexes.

Representative deposition conditions are listed in Table I. In our horizontal laminar-flow CVD reactor, the reagent mixture was depleted as it progressed through the reaction chamber. Thus, deposits were not uniform in thickness; they were thicker close to the inlet, and the thickness decreased along the length of the reactor. The thickness profile and the extent of coverage were dependnet on both the carrier gas flow rate and the deposition temperature. Increasing the deposition temperature caused the films to grow closer to the inlet of the CVD chamber and to cover a smaller area. Increasing the carrier gas flow rate produced coatings of more uniform thickness on a larger area, but higher carrier gas flow also promoted powder formation. The powder caused pinholes and cracks to form in the coatings, probably due to turbulences in the flow. The flow rates listed in Table I permitted the deposition of titanium nitride coatings that covered a 4 × 10 cm substrate.

Table II. Carbon Content of Titanium Nitride Films Deposited from $Ti(NMe_2)_4$ and NH_3 on Silicon as a Function of Deposition Temperature

deposition temp, °C	C/Ti ratio	deposition temp, °C	C/Ti ratio
200	<0.02	350	0.11
250	0.05	400	0.11–0.2
300	0.09		

The diameter of the delivery line had little effect on the titanium nitride deposits. The growth rates in this case were solely dependent on the vapor pressure of $Ti(NMe_2)_4$ and could be increased simply by heating the carrier gas and precursor feed line with heating tape. When $Zr(NEt_2)_4$ or $Hf(NEt_2)_4$ and NH_3 were used as precursors, the internal diameter of the $M(NR_2)_4$/He mixture delivery line significantly affected the film growth rates with a 2-mm-i.d. line producing a higher growth rate than a 1-mm-i.d. line. With the use of a 2-mm-i.d. delivery line, however, the zirconium and hafnium nitride deposits grew closer to the inlet of the CVD chamber and were less uniform in thickness than when the 1 mm line was employed. Higher carrier gas flow rates could be used to compensate for this effect. Heating the metal precursor feed line increased the zirconium and hafnium nitride film growth rates.

In comparison experiments, it was found that at the same carrier gas-flow rates and substrate temperatures, the zirconium and hafnium nitride films deposited closer to the inlet than the titanium nitride films. Also, the zirconium and hafnium nitride deposits covered a smaller area and were less uniform in thickness.

Titanium nitride films up to 2000 Å thick were grown. Attempts to grow films thicker than 2000 Å resulted in film cracking and powder formation. Zirconium and hafnium nitride films up to 5000 Å thick were grown with no cracking or powder formation observed.

Composition. Nitrogen-to-metal ratios were determined by Rutherford backscattering spectrometry (RBS), but RBS was not sensitive enough to detect the generally low levels of carbon and oxygen in the films. For this reason, X-ray photoelectron spectroscopy (XPS), a more sensitive technique than RBS for light element detection, was used to estimate carbon and oxygen contamination. XPS was not used to determine N/M ratios because of preferential sputtering of nitrogen (zirconium and hafnium nitride) and asymmetry in the metal electron peaks that made accurate integrations difficult (all cases).

Titanium Nitride. According to the RBS data, the titanium nitride films had N/Ti ratios of 1.05–1.15; that is, the stoichiometries were close to TiN (Figure 2a). Carbon and oxygen contamination was below the detection limits of RBS indicating that these elements were present at less than 2–3 atom %.

XPS analyses revealed that the surfaces of the films were covered with a layer (ca. 50 Å thick) that contained large amounts of carbon and oxygen. This layer resulted from the routine handling of the films in air after deposition. The oxide/carbon laden layer could be removed completely by sputtering for 1–2 min with a 3-keV Ar^+ gun. XPS depth profile data indicated that the amount of oxygen in the bulk of the films was less than 1 atom % when depositions were carried out below 250 °C. The data also showed that the films were uniform in composition. Carbon contamination in the films increased as the temperature of deposition increased (Table II). Films deposited above 350 °C contained as much as 5 atom %

(69) Sugiyama, K.; Pac, S.; Takahashi, Y.; Motojima, S. *J. Electrochem. Soc.* **1975**, *122*, 1545. See also: Kutyreva, V. V.; Varyukin, V. A.; Suvorova, O. N.; Nesterov, B. A.; Domrachev, G. A. *Izv. Akad. Nauk. SSSR, Neorg. Mater.* **1979**, *15*, 1692; *Chem. Abstr.* **1979**, *91*, 179577x.

(70) The preparation of thin films from titanium complexes with other types of nitrogen-bearing ligands: Morancho, R.; Constant, G.; Ehrhardt, J. J. *Thin Solid Films* **1981**, *77*, 155; Morancho, R.; Constant, G. C. R. *Acad. Sci. Ser. C* **1977**, *285*, 77; Morancho, R.; Petit, J. A.; Dabosi, F.; Constant, G. *J. Electrochem. Soc.* **1982**, *129*, 854.

(71) Hilton, M. R.; Vandentop, G. J.; Salmeron, M.; Somorjai, G. A. *Thin Solid Films* **1987**, *154*, 277.

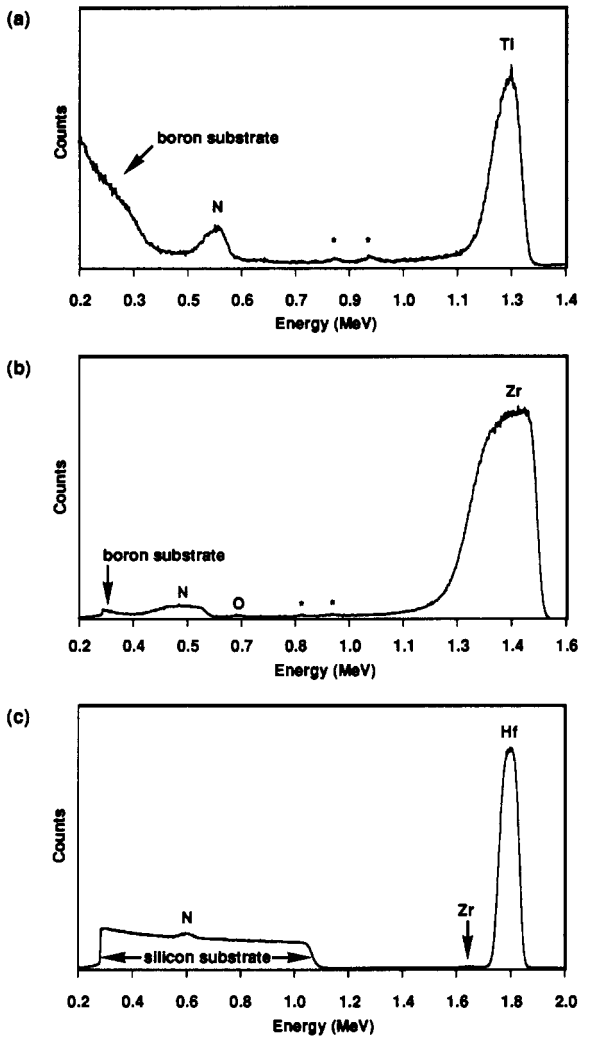

Figure 2. Rutherford backscattering spectra for titanium nitride (a), zirconium nitride (b), and hafnium nitride (c) films deposited from $M(NR_2)_4$ (M = Ti, R = Me; M = Zr or Hf, R = Et) and ammonia at 200 °C. The substrates in (a) and (b) were boron disks; the starred peaks and the oxygen peak in (b) were present in spectra run for the blank substrates prior to deposition. For (c) the substrate was silicon; the zirconium signal arises from the $ZrCl_4$ impurity present in the $HfCl_4$ used in the preparation of $Hf(NEt_2)_4$.

carbon. The highest purity films were obtained at 200 °C; they contained less than 1 atom % carbon and oxygen.

Zirconium and Hafnium Nitride. RBS analyses showed that the zirconium nitride films deposited in the temperature range 200–400 °C had a nitrogen-to-metal ratio of 1.35 ± 0.05 (Figure 2b). This ratio is consistent with the phase Zr_3N_4. The hafnium nitride films had a N/M ratio of 1.7 ± 0.1 (Figure 2c). This ratio and the physical properties displayed by the material are consistent with a Hf_3N_4 phase in which an excess of nitrogen is incorporated. For both the zirconium and hafnium nitride films, the stoichiometries were independent of the deposition temperature.

No carbon or oxygen was detected in the zirconium or hafnium nitride films by RBS. XPS depth profile data showed that, in general, these films contained less than 1 atom % of carbon and oxygen. In contrast to the titanium nitride coatings, the carbon content in the zirconium and hafnium nitride films did not change with deposition temperature.

Hydrogen Content. Hydrogen forward recoil scattering (FRS) spectrometry was used to estimate the amount of hydrogen in the films.[67] Table III summarizes the data.

Table III. Hydrogen-to-Metal Ratios for Titanium, Zirconium, and Hafnium Nitride Films Deposited on Silicon as a Function of Deposition Temperature[a]

deposition temp, °C	H/Ti	H/Zr	H/Hf
150	1–1.1		
200	0.60–0.65	0.9–1.0	1.25–1.35
300	0.40–0.45	0.25–0.30	0.50–0.55
400	0.20–0.25		0.05–0.15

[a] See the Experimental Section for details concerning data collection and analysis.

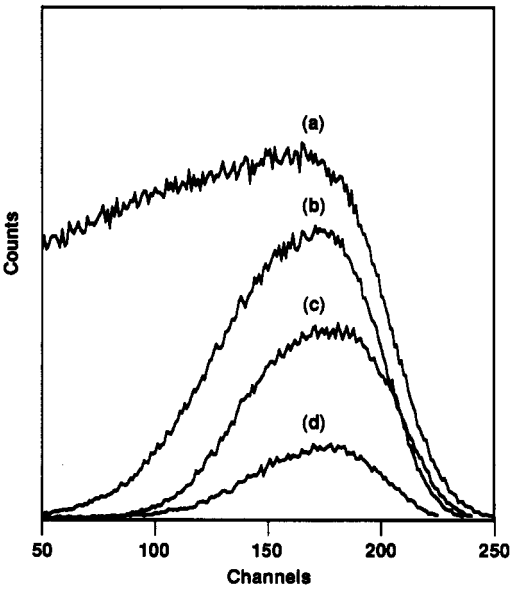

Figure 3. Hydrogen forward recoil scattering spectra for gypsum (a) and titanium nitride films deposited at 150 (b), 200 (c), and 400 °C (d) on silicon substrates.

The FRS spectra of TiN films deposited at temperatures ranging from 150 to 400 °C are shown in Figure 3. Analysis of the spectra indicated that the hydrogen content was temperature dependent; films deposited at 150 °C contained approximately 33 atom % hydrogen, whereas films deposited at 400 °C contained about 10 atom % hydrogen. It was noteworthy that even though the films were hydrogenated, they were not air-sensitive and were stable to common inorganic acids.

Analysis of the forward recoil scattering spectra for zirconium and hafnium nitride films showed that the hydrogen content was also temperature dependent in these films. Interestingly, at 200 °C the hafnium and zirconium nitride coatings contained more hydrogen than the titanium nitride films, whereas at higher temperatures the opposite was observed.

Microstructure. All of the films were featureless by scanning electron microscopy. We therefore used transmission electron microscopy (TEM) to examine thin films (about 300 Å thick) that had been deposited on carbon-coated mica. The micrographs revealed that the films were crystalline as deposited.[61]

The films had a granular structure with poorly defined grain boundaries. The grain size was 2–5 nm for the titanium nitride coatings and even smaller (<2 nm) for the zirconium and hafnium nitride films.[61] The temperature of deposition did not affect the grain sizes, but higher temperatures did produce films with better defined grains.

Crystal Structure. Because of the size of the microcrystallites, it was not possible to obtain single-crystal diffraction data. Selected area electron diffraction for

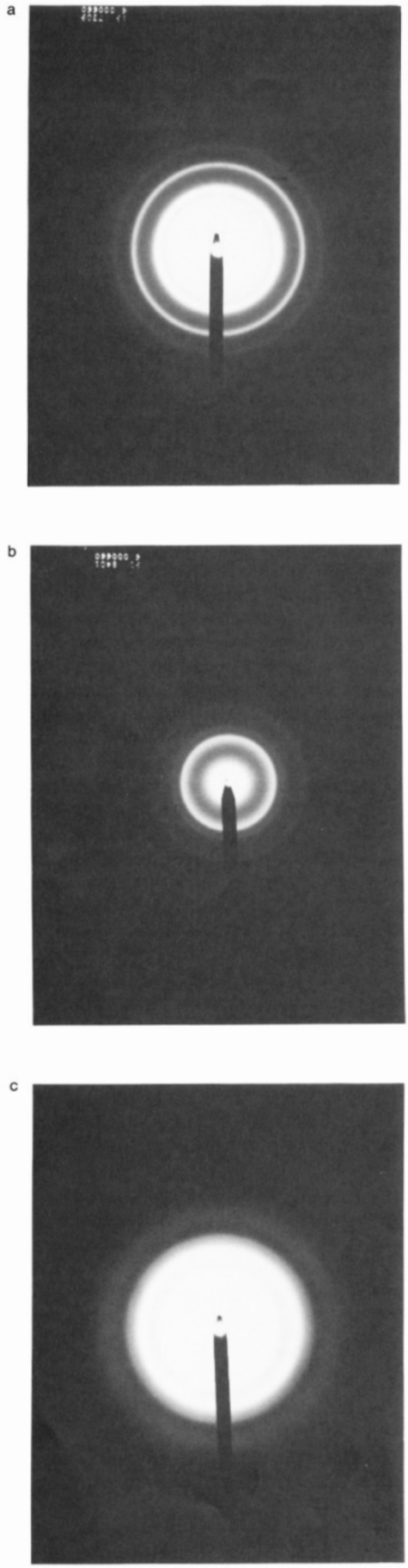

Figure 4. Selected area electron diffraction pattern of titanium (a) and zirconium (b) nitride films deposited at 200 °C and hafnium nitride (c) deposited at 400 °C on carbon-coated mica.

Table IV. X-ray Photoelectron Spectroscopy Binding Energies (eV) for Films Deposited on Silicon at 200 °C[a]

film	metal binding energy (assignment)	N 1s binding energy
TiN	454.8 (Ti $2p_{3/2}$)	396.9
Zr_3N_4	180.3 (Zr $3d_{5/2}$)	397.2
Hf_3N_4	15.1 (Hf $4f_{7/2}$)	397.0

[a] The error in the binding energies is estimated to be ±0.2 eV.

titanium and zirconium nitride coatings deposited at 200 °C, however, produced sharp ring patterns (Figure 4a,b). A diffraction pattern for the hafnium nitride film deposited at 200 °C showed more diffuse rings. This was probably due to the smaller grain size. A sharper diffraction pattern for hafnium nitride was obtained for a film deposited at 400 °C (Figure 4c).

Titanium Nitride. The mononitrides TiN, ZrN, and HfN all have a fcc NaCl-type structure.[2] The diffraction pattern obtained for our titanium nitride film was consistent with that reported in the powder diffraction file for cubic *Fm3m* (225) TiN.[72] The electron diffraction pattern did not indicate any preferential orientation. The lattice parameter was 4.24 (1) Å, which is consistent with the reported value for bulk TiN.[72]

Zirconium Nitride. The diffraction pattern for zirconium nitride was similar to the one reported for the ZrN *Fm3m* (225) structure,[73] but the ring corresponding to the (111) reflection was broader, asymmetric and shifted to higher d_{111} spacings (the other reflections were normal). These features have been shown to be characteristic of the Zr_3N_4 structure.[39,41] Johansson and co-workers,[39] who deposited nitrogen-rich zirconium nitride films by dual ion beam deposition, have rationalized these features as arising from a rhombohedral distortion of the cubic lattice in order to acommodate the excess of nitrogen. The broadening of the (111) reflection was thought to be due to the appearance of a new peak.

The (111) reflection was strong and the (200) reflection was weak in our zirconium nitride films. This suggests a strong preferential orientation, which is common for thin films. A similar preferential orientation was observed for Zr_3N_4 by Ristolainen and co-workers[41] and Johansson and co-workers.[39] Structural assignments cannot be based on relative intensities because of the preferential orientation.

On the basis of the (200) and (220) reflections, we calculated a lattice parameter of 4.59 (1) Å for Zr_3N_4 which is close to the value reported for bulk ZrN (4.574 Å). The cell parameter was 4.63–4.70 Å based on the (111) reflection. The large error was due to the broadness of the (111) reflection. The lattice parameters were in accord with those determined by Ristolainen and co-workers for their Zr_3N_4 films (4.60 and 4.65 Å based on the (200) and (111) reflections, respectively).[41]

Hafnium Nitride. The diffraction pattern for a hafnium nitride film deposited at 420 °C showed the broadening and shift of the (111) reflection characteristic of the Hf_3N_4 phase.[39] The high intensity of the (111) reflection indicated the films had a (111) preferred orientation. The lattice parameter was 4.50–4.55 Å based on the (200) reflection. Stoichiometric HfN has a cell constant of 4.52, and Johansson and co-workers reported a value of 4.54 Å for sputtered hafnium nitride films in which there was an

(72) TiN: Index card No. 38-1420. *Powder Diffraction File*; McClune, W. F., Ed.; JCPDS International Center for Diffraction Data: Swarthmore, PA.

(73) ZrN: Index Card Nos. 35-753, 31-1493. *Powder Diffraction File*; McClune, W. F., Ed.; JCPDS International Center for Diffraction Data: Swarthmore, PA.

Table V. Selected Physical Properties of the Group IV Nitride Films

coating	resistivity,[a] μΩ cm	optical band gap,[b,c] eV	refractive index[d]
TiN	≈10^3		
Zr_3N_4	>10^6	2.2[d]	2.9–3.3
Hf_3N_4	>10^6	2.7[d]	2.4–2.8

[a] Films deposited on 7059 glass at 200–400 °C. [b] Films deposited on 7059 glass at 200 °C. [c] The error for these numbers is estimated to be ±0.2 eV. [d] Films deposited on Si at 200–400 °C.

excess of nitrogen.[11] Because of the diffuse nature of the (111) reflection, it was not possible to evaluate a cell constant based on this reflection.

Bonding by XPS Analysis. Experimental binding energies are presented in Table IV.

Titanium Nitride. After removal of the surface oxide layer by sputtering for 2–5 min with a 2-keV Ar^+ gun, the binding energies of the Ti $2p_{3/2}$ and N 1s lines were determined to be 454.8 and 396.9 eV, respectively. These numbers were in good agreement with those obtained in an exhaustive XPS study of TiN_x carried out by Baiocchi and co-workers.[74] Our values were independent of the deposition temperature. They were reproducible to ±0.2 eV and remained constant throughout the sample as indicated by XPS depth profile data.

The N 1s peak was sharp and the Ti 2p peak was asymmetrical with a strong shoulder at 456 eV. Baiocchi and co-workers have studied in detail the trailing and shoulder intensity of the Ti $2p_{3/2}$ peak as a function of N and O content for TiN_x films.[74] They found that an increase in the concentration of these elements resulted in increased intensity of the shoulder. On the basis of this study and the fact that our films were shown to be nearly oxygen-free by XPS and RBS analyses, the Ti 2p line shape suggests a slightly nitrogen-rich material. This is consistent with the N/Ti ratio of 1.10 obtained by RBS.

It was noteworthy that no preferential sputtering was observed while depth profiling the TiN films. Also, the XPS composition data yielded a higher N/Ti ratio than the RBS analysis (1.3 vs 1.1), which is undoubtedly a consequence of the Ti 2p line shape. A similar effect was encountered by Baiocchi and co-workers.[74]

Zirconium Nitride. XPS studies for Zr_3N_4 revealed binding energies of 180.3 eV for the Zr $3d_{5/2}$ line and 397.2 eV for the N 1s line. The binding energy of the Zr line was identical to the one reported by Netterfield and co-workers[40] for Zr_3N_4 prepared by ion-beam-assisted deposition and the line shape, which was asymmetrical, was also similar. The Zr $3d_{5/2}$ binding energy for Zr_3N_4 is slightly higher than the values reported for ZrN.[40,75,76]

The N 1s binding energy was similar to the values usually found for early transition-metal nitrides and ZrN (396.3–397.5 eV) in particular[75,76] but was slightly different from Netterfield and co-workers value for Zr_3N_4 (396.3 eV).[40]

Hafnium Nitride. The Hf $4f_{7/2}$ and N 1s binding energies were 15.1 and 397.0 eV, respectively. These values were consistent with those reported by Perry and co-workers for HfN (15.2–15.7 and 397.5 eV, respectively).[77] The Hf 4f line was asymmetrical.

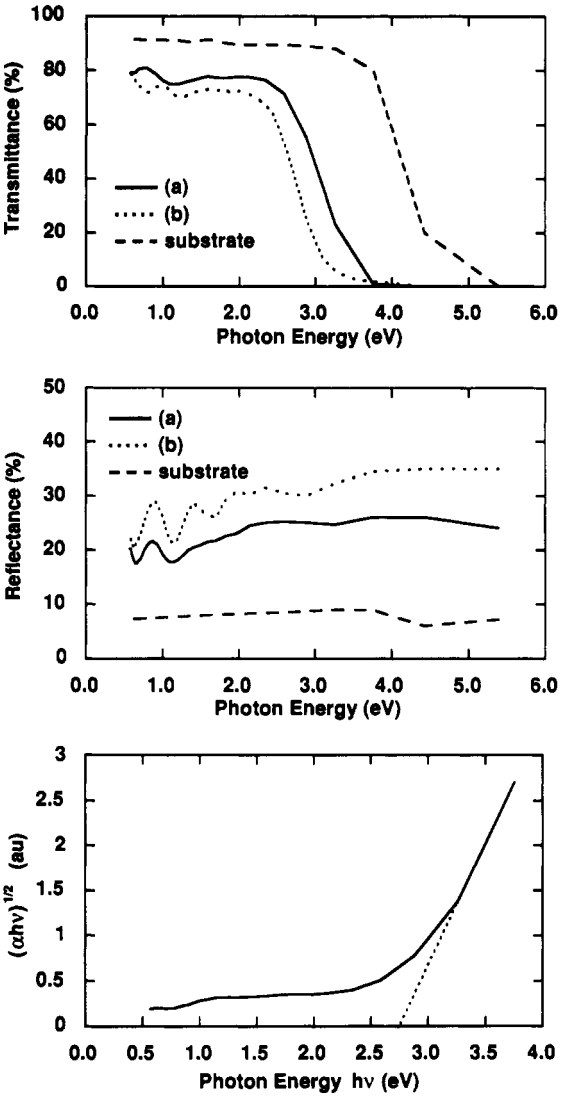

Figure 5. Top: transmission spectra for hafnium nitride thin films (≈5000 Å thick) deposited at 200 (a) and 300 °C (b) on 7059 glass substrates. Middle: reflectance spectra of hafnium nitride thin films (≈5000 Å thick) deposited at 200 (a) and 300 °C (b) on 7059 glass substrates. Bottom: $(\alpha h\nu)^{1/2}$ vs $h\nu$ (solid line) for a hafnium nitride film deposited on 7059 glass at 200 °C. The dotted line represents the best fit for the linear portion of the curve.

Electrical and Optical Properties. The electrical and optical properties of the films are summarized in Table V. The transmission and reflectance spectra of hafnium nitride films of approximately the same thickness prepared at different temperatures are shown in Figure 5. The spectra show a dependence on the temperature of deposition, which is common for films prepared by CVD. Transmission and reflectance spectra for the titanium and zirconium nitride films were also recorded.

Optical Bandgap. The optical bandgaps for the zirconium and hafnium nitride films were obtained from optical transmission measurements by plotting $(\alpha h\nu)^{1/2}$ vs $h\nu$, where α is the absorption coefficient ($\alpha = -\log T/T_0$; T, sample optical transmission; T_0, substrate optical transmission) and $h\nu$ the photon energy (e.g., Figure 5).[45,78] The plots showed $(\alpha h\nu)^{1/2}$ was linearly dependent on $h\nu$ for $h\nu$ greater than the bandgap. This type of function is normally observed for materials with an indirect bandgap

(74) Vasile, M. J.; Emerson, A. B.; Baiocchi, F. A. *J. Vac. Sci. Technol. A* **1990**, *8*, 99.
(75) Höchst, H.; Bringans, R. D.; Steiner, P.; Wolf, T. *Phys. Rev. B* **1982**, *25*, 7183.
(76) Konuma, M.; Matsumoto, O. *J. Less Common Met.* **1977**, *56*, 129.
(77) Perry, A. J.; Schlapbach, L.; Sproul, W. D. *Solid State Commun.* **1987**, *62*, 23.
(78) Tauc, J.; Grigorovici, R.; Vancu, A. *Phys. Status Solidi* **1966**, *15*, 627.

and bands that are free-electron-like.[78] An extrapolation of the linear portion of the curve to $\alpha = 0$ gave the optical bandgap at the intercept of the abscissa. In this way, optical band gaps of 2.2 and 2.7 eV for zirconium and hafnium nitride respectively, were calculated. These values should be interpreted with caution because α was not corrected for interference effects due to reflection.

Resistivity. Sheet resistances were obtained for coatings deposited on 7059 glass by using the four-point probe method. The resistivity was obtained by multiplying the sheet resistance by the film thickness obtained from RBS analysis. For TiN films deposited between 200 and 400 °C, the resistivity was approximately 10^3 $\mu\Omega$ cm. The resistivity was not dependent on the temperature of deposition. The zirconium and hafnium nitride films were insulating (sheet resistances >100 kΩ/square).

Refractive Index. Refractive indexes were obtained by using a fixed-wavelength (6228 Å) ellipsometer (Rudolf Auto-E1 II). In all cases, the refractive indexes were not dependent on the temperature at which the films were deposited. For the zirconium nitride films the refractive indexes were in the range 2.9–3.3. These values are in good agreement with those reported in the literature.[19,40] The indexes were strongly dependent on oxygen content; for example, the indexes were 2.15–2.25 for zirconium nitride films containing 10 atom % oxygen. The refractive indexes of hafnium nitride films (<3 atom % O) were 2.4–2.8. They varied with the film thickness.

Discussion

Titanium Nitride. $Ti(NMe_2)_4$ and ammonia precursors deposited high-purity TiN films at remarkably low temperatures (150–450 °C). RBS analyses showed that the films were slightly nitrogen-rich with a N/Ti ratio of ca. 1.1. The N/Ti ratios were independent of the temperature of deposition. XPS analyses of the films were also consistent with a slightly nitrogen-rich TiN. FRS analyses revealed that the films were hydrogenated, with the hydrogen content decreasing with increasing deposition temperature (see below). The highest purity films were deposited at 200 °C where the C and O contamination was less than 1 atom %.

The TiN films were crystalline as deposited at 200 °C with 2–5-nm microcrystallites. They exhibited sharp electron diffraction patterns that were consistent with the TiN cubic phase. The crystallinity was somewhat surprising because most CVD coatings deposited at very low temperatures, for example, TiC deposited at 150–400 °C from $Ti(CH_2\text{-}t\text{-}Bu)_4$[79] and AlN deposited at 400–600 °C from $[Al(CH_3)_2NH_2]_3$[80] or $[Al(CH_3)_2N_3]_3$,[81] were amorphous and postdeposition annealing was required to form crystalline material. The crystallinity of our deposits suggests that the depositing species had mobility at the gas–surface interface of the growing film.

The cell parameter for our slightly nitrogen-rich TiN was close to the reported values for stoichiometric TiN. Interestingly, Noël and co-workers observed an increase in the cell parameter for their slightly nitrogen-rich titanium nitride.[34] They proposed that the increase was due to a filling of the tetrahedral interstices. Because no lattice expansion was observed for our films, we suggest a crystal structure with metal sites vacancies as proposed by Sundgren and co-workers for a similar material.[82]

Our TiN films were electrical conductors with resistivities around 10^3 $\mu\Omega$ cm. The resistivity of bulk TiN is 22 $\mu\Omega$ cm,[2] but this value is seldom attained in thin films. TiN coatings prepared by CVD usually have resistivities ranging from 200 to 6000 $\mu\Omega$ cm.[18] The lowest resistivities in TiN thin films (100–200 $\mu\Omega$ cm) are usually oberved for stoichiometric TiN prepared by reactive sputtering. Substoichiometric and overstoichiometric titanium nitride coatings prepared by physical vapor deposition techniques have higher resistivities (200–500 $\mu\Omega$ cm).[21] The resistivity of TiN also increases sharply with oxygen, carbon, or chloride contamination. In our case these impurities were either absent entirely or present in very low concentrations. The high resistivity we observed could be due to the slight excess of nitrogen, the hydrogen content, or the small grain size.

The method we have developed for the deposition of TiN has advantages over processes employing $TiCl_4$ and N_2/H_2 or ammonia. An obvious advantage is the lower deposition temperatures, which permit depositions on highly thermally sensitive substrates (e.g., plastics and computer microcircuits). Also, unlike the conventional processes, our system produces no corrosive HCl byproduct, which is undesirable in technological applications. Chloride contamination in TiN films has caused adhesion problems to stainless steel substrates.[18] No adhesion problems were encountered with the use of the $Ti(NMe_2)_4/NH_3$ system.

Zirconium and Hafnium Nitrides. Our low-temperature process involving the reaction of $M(NEt_2)_4$ compounds and ammonia produced crystalline nitride films that had N/M ratios of 1.35 and 1.7 for M = Zr and Hf, respectively. These ratios are consistent with stoichiometric Zr_3N_4 and nitrogen-rich Hf_3N_4 phases. The N/M ratios did not depend on deposition temperature, but the hydrogen content decreased as the deposition temperatures were increased, (see below). In contrast to group 4 MN films, the M_3N_4 films were transparent and insulating, consistent with earlier reports.

Selected area electron diffraction for the zirconium and hafnium nitride films revealed a ring pattern similar to those reported for ZrN and HfN, but with an increase in the d_{111} spacings. This feature had been previously noted for Zr_3N_4 and Hf_3N_4 films and was explained as arising from a rhombohedral distortion of the NaCl lattice. Johansson and co-workers proposed that the distortion was due to a filling of the smaller vacant tetrahedral interstices of the lattice with nitrogen.[39] On the other hand, Schwartz and co-workers proposed an ordered structure based on metal site vacancies.[52] In general, early transition-metal nitrides have vacancies in their structure even when stoichiometric.[2] It is likely our materials have both vacant metal sites and partially filled tetrahedral interstices.

Zr_3N_4 powder was first prepared from ZrI_4 and NH_3 by Juza and co-workers.[53] Hf_3N_4 has apparently never been prepared by any chemical route. Previous CVD routes to zirconium and hafnium nitrides used the metal halides and N_2/H_2 or NH_3 precursors. These reactions required high temperatures, and only the thermodynamically stable mononitride phase was obtained. Lower reaction temperatures did allow formation, however, of halogen-contaminated powders in which some Zr_3N_4 could be detected.[55] The actual preparations of high-quality Zr_3N_4 and Hf_3N_4 thin films was only recently achieved by physical deposition techniques. To our knowledge this report is the

(79) Girolami, G. S.; Jensen, J. A.; Pollina, D. H.; Allocca, C. M.; Kaloyeros, A. E.; Williams, W. S. *J. Am. Chem. Soc.* **1987**, *109*, 1579.
(80) Interrante, L. V.; Lee, W.; McConnel, M.; Lewis, N.; Hall, E. *J. Electrochem. Soc.* **1989**, *136*, 472.
(81) Boyd, D. C.; Haasch, R. T.; Mantell, D. R.; Schulze, R. K.; Evans, J. F.; Gladfelter, W. L. *Chem. Mater.* **1989**, *1*, 119.
(82) Sundgren, J.-E.; Johansson, B.-O.; Karlsson, S.-E.; Hentzell, H. T. G. *Thin Solid Films* **1983**, *105*, 367.

first concerning the CVD preparation of Zr_3N_4 and Hf_3N_4 thin films.

Hydrogen Content, Microstructure, and Bonding. All of the films were hydrogenated. The hydrogen content of the films decreased as the temperature of deposition increased. Titanium nitride films deposted at 150 °C contained 33 atom % hydrogen, which suggests a composition close to TiNH. When deposited at 200 °C the titanium nitride film composition was close to $TiN_{1.1}H_{0.6}$, and at 400 °C the films had a $TiN_{1.1}H_{0.2}$ formula. Zirconium and hafnium nitride films deposited at 200 °C had the compositions $ZrN_{1.35}H_{0.9}$ and $HfN_{1.7}H_{1.35}$. At 300 °C the stoichiometries were $ZrN_{1.35}H_{0.25}$ and $HfN_{1.7}H_{0.5}$.

How is the hydrogen and the excess nitrogen bound in the films? By analogy to solution chemistry,[57-60] there are probably NH and NH_2 groups in the materials. The excess nitrogen in TiN and Hf_3N_4 suggests that N-N bonds may be present.

How are the putative NH, NH_2, and N–N groups incorporated in the films? There are two possibilities: Either the groups are located within the crystallites or at the grain boundaries between the crystallites of TiN or M_3N_4. The latter is a more satisfactory explanation because each of the films revealed diffraction patterns consistent with stoichiometric phases; that is, the diffraction patterns showed that the titanium nitride had a cubic TiN structure and the zirconium and hafnium nitrides had the M_3N_4 structure. It is therefore reasonable to speculate that our materials were composed of TiN or M_3N_4 grains, which gave the characteristic diffraction patterns, imbedded in an amorphous material in which NH, NH_2, and possibly N–N groups were present.

Solution-Phase Reactivity and Periodic Trends. The basis for our choice of precursors was kinetically facile solution reactions, transamination (eq 3) and amine elimination reactions (eqs 4 and 5), that suggested similar facile reactions would occur in CVD reactions. The reactions leading to the nucleation of the metal nitrides are certainly more complex than the simple transamination and amine elimination reactions might suggest, but the experimental observations that follow are consistent with reactions occurring in the gas phase that are similar to those in solution.

(1) The growth rates of the zirconium and hafnium nitride films were higher and the films deposited closer to the reactor inlet and covered a smaller area than the TiN films. These facts suggest a faster reaction of ammonia with $Zr(NEt_2)_4$ and $Hf(NEt_2)_4$ than with $Ti(NMe_2)_4$. This is consistent with an associative mechanism between ammonia and the metal complexes: Hf and Zr are larger than Ti, and therefore the approach of NH_3 to the metal center for these elements is easier, even though bulkier alkyl groups are present on the amido ligands of the Zr and Hf complexes (Et vs Me).

(2) The films were free of carbon contamination. This suggests that all of the NR_2 ligands were replaced by NH_2, NH, or N groups, via amine elimination reactions, before the depositing species found the film surface.

It should also be noted that in no case was substrate selectivity observed, and there was formation of a large amount of powder on the top wall of the reactor. This and the fact that the film thickness profiles depended on the carrier gas flow rate, suggest that the nucleation and deposition processes were controlled by gas-phase reactions, which is typical of atmospheric pressure CVD processes.

These observations suggest that the early stages of the CVD reactions proceed according to the pathways illustrated by eqs 6 and 7.

$$M(NR_2)_4 + NH_3 \rightarrow M(NR_2)_{4-n}(NH_2)_n + nHNR_2 \quad (6)$$

$$M(NR_2)_{4-n}(NH_2)_n \longrightarrow M(NH_m)_x \longrightarrow MN_z \quad (m = 0, 1, \text{or } 2) \quad (7)$$

The steps in eq 6 involve the substitution of one or more NR_2 (R = Me or Et) ligands by NH_2 groups via reactions with ammonia. In eq 7, the NH_2-substituted product then eliminates the remaining NR_2 groups via α-hydrogen activation reactions involving NH_2 ligands, thereby leaving imido M=NH groups and, subsequently, nitrido MN linkages.

In addition to reactions 3–5, there are other precedents for reactions 6 and 7 from solution studies of group 4 compounds. For example, Maya and Brown showed that ammonolysis of $Ti(NMe_2)_4$ led to a polymeric material for which the formula "Ti_3N_4" was proposed.[83] Subsequent pyrolysis at 800 °C of the polymer led to TiN. Other evidence for the displacement of NR and NR_2 groups by NH_3 was given by Seyferth and Mignani's study of the pyrolysis of oligomeric titanium amido and imido compounds in an ammonia stream.[84]

It is interesting that the reaction of $Ti(NMe_2)_4$ and ammonia led to TiN, indicating a formal reduction from Ti^{IV} in the precursor to Ti^{III} in the film. The mechanism of this reduction is not known, but it is perhaps accomplished via Ti–N homolytic bond cleavage,[85] which would produce a NR_2 or NH_2 radical and the required Ti^{III} center. Homolytic Ti–N bond cleavage was proposed in the decomposition of cyclic amido complexes in which there was no evidence for β-hydrogen activation.[85] The contrasting chemistry between titanium, a first-row transition element, and the heavier elements zirconium and hafnium, for which the tetrakis(dialkylamido) compounds did not show a reduction during deposition, can be rationalized on the basis of periodic trends; that is, the heavier metal $M(NR_2)_4$ compounds are more difficult to reduce.

We observed an increase in carbon contamination of the TiN films with deposition temperature. This was most likely the result of intramolecular dimethylamido β-hydrogen activation, which occurred more readily at high temperatures and effectively competed with the inter- and intramolecular deposition chemistry. There was no similar increase in carbon contamination with higher deposition temperatures for the zirconium and hafnium nitride films. A possible explanation is a higher reactivity of the larger metal center toward ammonia, which precluded competing intramolecular diethylamido β-hydrogen activation.

The chemical vapor deposition of TiN thin films from $TiCl_4$ and NH_3 and the synthesis of powders containing Zr_3N_4 by the vapor phase reaction of $ZrCl_4$ with NH_3 are high-temperature processes (>550 °C). Why do the dialkylamido precursors allow a much lower temperature of deposition? The M–Cl bonds in MCl_4 (M = Ti, Zr, Hf) compounds are approximately 20 kcal/mol stronger than the M–N bonds in $M(NR_2)_4$ compounds.[86] Thus, the $M(NR_2)_4$ compounds would thermodynamically favor nitride formation relative to MCl_4 compounds. Also, in our process, the precursors were selected because of their expected facile reactions with ammonia; in solution they readily underwent transamination and amine elimination reactions. We assumed that in the gas phase the $M(NR_2)_4/NH_3$ precursors would rapidly generate M–NH_2

(83) Brown, G. M.; Maya, L. *Abstracts of Papers*, 199th National Meeting of the American Chemical Society, Boston, MA; American Chemical Society: Washington, DC, 1990; INOR 118.
(84) Seyferth, D.; Mignani, G. *J. Mater. Sci. Lett.* **1988**, *7*, 487.
(85) Fix, R.; Gordon, R. G.; Hoffman, D. M. *Chem. Mater.* **1990**, *2*, 235.
(86) Lappert, M. F.; Patil, D. S.; Pedley, J. B. *J. Chem. Soc., Chem. Commun.* **1975**, 830.

species. The vapor-phase reaction of MCl_4 and NH_3 at low temperature (<200 °C) are reported to produce $MCl_4 \cdot xNH_3$ adducts.[55,87-89] These adducts are undoubtedly less reactive than the putative NH_2-substituted compounds. Our system is therefore also kinetically more labile than the MCl_4/NH_3 system.

Conclusion

We have prepared high-quality TiN, Zr_3N_4, and Hf_3N_4 thin films from tetrakis(dialkylamido)metal(IV) complexes and ammonia precursors with high growth rates at low temperatures (200-450 °C). The TiN and Hf_3N_4 were slightly nitrogen rich. The TiN films displayed metallic properties and were crystalline as deposited. The Zr_3N_4 and Hf_3N_4 films were crystalline, yellow, transparent, and insulating. Periodic trends can be used to rationalize the contrasting result that Ti(III) films deposited from Ti(IV) precursors whereas Zr(IV) and Hf(IV) films deposited from Zr(IV) and Hf(IV) precursors.

Acknowledgment. We thank the National Science Foundation (DMR-88-02306) for supporting this work, and the Department of Energy for an instrumentation grant (DE-FG05-86ER85287). We thank Yuan Z. Lu for his help in obtaining the TEM data. The RBS spectra were acquired by using the Cambridge Accelerator for Materials Sciences housed in the Harvard Materials Research Laboratory, an NSF-funded facility (DMR-86-14003). D.M.H. thanks the Robert A. Welch Foundation for support in the latter stages of this research.

Registry No. TiN, 25583-20-4; Hf_3N_4, 104382-33-4; Zr_3N_4, 12033-93-1.

(87) Fowles, G. W. A.; Pollard, F. H. *J. Chem. Soc.* **1953**, 2588.
(88) Antler, M.; Laubengayer, A. W. *J. Am. Chem. Soc.* **1955**, *77*, 5250.
(89) Hojo, J.; Kato, A. *Yogyo-Kyokai-Shi* **1981**, *89*, 277.

Amorphous Alloy Thin Films from Molecular Precursors. Evidence of Structure and Stoichiometry from Crystallization and Effects of Precursor Ligand Structure on Stoichiometry

B. H. S. Thimmappa and Thomas P. Fehlner*

Department of Chemistry, University of Notre Dame, Notre Dame, Indiana 46556

Gary J. Long* and O. Allan Pringle

Departments of Chemistry and Physics, University of Missouri—Rolla, Rolla, Missouri 65401

Received August 13, 1991

The crystallization at 400 °C of amorphous thin films formed by the thermal decomposition of $HFe_3(CO)_9BH_4$ at low low pressure has been studied by using the techniques of X-ray diffraction and Mössbauer spectroscopy. The results unambiguously show that the films are iron rich in terms of the ideal stoichiometry of Fe/B = 3, signifying some loss of boron during film formation. The iron-main group atom phase that crystallizes from the amorphous film is orthorhombic $Fe_3B_{1-x}C_x$, with x for the specific film examined lying between 0.3 and 0.4. The cleavage of CO is postulated to account for the overall Fe/B ratio of 3, formation of the mixed boride/carbide phase and the presence of B_2O_3 in the film. That is, the boron sequesters the oxygen atom as B_2O_3, whereas the carbon atom replaces boron so lost in Fe_3B to form the $Fe_3B_{1-x}C_x$ phase. Deposition of films from a closely related precursor, $HFe_3(CO)_{10}BH_2$, have also been examined. Most of the boron is lost during deposition even at the lowest substrate temperature. Crystallization of these amorphous films requires higher temperatures and yields α-Fe and a phase indistinguishable from orthorhombic Fe_3C. Decomposition during sublimation with the production of $Fe(CO)_5$ accounts for the qualitatively different behavior of $HFe_3(CO)_{10}BH_2$.

Introduction

We have previously described the thermal decomposition of $HFe_3(CO)_9BH_4$ at 175-200 °C and low pressures at the surface of various substrates. The result was the deposition of uniform, thin, amorphous alloy films of approximate composition $Fe_{75}B_{25}$.[1] Apparently the ligands of $HFe_3(CO)_9BH_4$ are lost as CO and H_2, and the Fe_3B core of the cluster is left as a solid deposit. The Mössbauer spectra of these films show that the local structure of the film is similar to that observed for films prepared by rapid quenching techniques but that the magnetically ordered films formed exhibit magnetic moments with a preferential orientation normal to rather than parallel with the film plane. This orientation is independent of the temperature. The films are stable in air, and the carbon and oxygen impurities found are known to be incorporated in the film during the deposition procedure. The oxygen appears to be present principally as B_2O_3, and as a result the Mössbauer spectra indicate that the films contain no ordered iron oxides.

Our earlier work raised a number of fundamental questions that required more experimental work and are answered herein. First, the spectroscopic analysis did not define the film composition with sufficient accuracy to prove that the ferraborane cluster core was deposited intact. Indeed there was an indication that the films had a Fe/B ratio somewhat higher than 3. Second, although oxygen impurities at low levels appeared to be tied up with

(1) Amini, M. M.; Fehlner, T. P.; Long, G. J.; Politowski, M. *Chem. Mater.* **1990**, *2*, 432.

0897-4756/91/2803-1148$02.50/0